CMR INSTITUTE OF TECHNOLOGY

USN | | | | | | | | | | |

Internal Assesment Test-I									
Sub:	Optical and Wireless Communication							Code:	21EC72
Date:	15/10/2024	Duration:	90 mins	Max Marks:	50	Sem:	4th	Branch:	ECE(A,B,C,D)
Answer any **FIVE FULL** Questions									

		Marks	OBE CO	OBE RBT
1.	a) What is the significance of cutoff wavelength and V number for optical fibers? b) An optical fiber has a core index of 1.480 and a cladding index of 1.478. What is the core size for single-mode operation at 1550 nm?	[05] [05]	CO1 CO1	L2 L3
2.	With optical ray diagram, define numerical aperture (NA) and state its significance. Derive the expression for NA and acceptance angle for single mode step index fiber.	[10]	CO1	L2
3.	Discuss the following for optical fibers: a) Fiber bending loss b) Scattering loss	[10]	CO1	L2
4.	Explain Intermodal dispersion with necessary equations.	[10]	CO1	L2
5.	Explain Fabry Perot resonator cavity of LASER with necessary diagrams and equations.	[10]	CO2	L2
6.	Explain internal quantum efficiency and power in detail for LED.	[10]	CO2	L2
7.	a. Consider a 30-km long optical fiber that has an attenuation of 0.4 dB/km at 1310 nm. Find the optical output power Pout if 200 mW of optical power is launched into the fiber.	[06]	CO1	L3
	b. Consider a multimode step-index optical fiber that has a core radius of 25 μm, a core index of 1.48, and an index difference Δ = 0.01. The number of modes M = 760. Find the percentage of optical power that propagates in the cladding at 840 nm.	[04]	CO1	L3

1. a) What is the significance of cutoff wavelength and V number for optical fibers? [05] CO1 L2
   b) An optical fiber has a core index of 1.480 and a cladding index of 1.478. What is the core size for single-mode operation at 1550 nm? [05] CO1 L3

a)

Guided modes in the fiber occur when the values for β satisfy the condition $n_2k < \beta < n_1k$. At the limit of propagation when $\beta = n_2k$, a mode is no longer properly guided and is called being *cut off*. Thus unguided or radiation modes appear for frequencies below the cutoff point where $\beta < n_2k$. However, wave propagation can still occur below cutoff for those modes where some of the energy loss due to radiation is blocked by an angular momentum barrier that exists near the core-cladding interface.[17] These propagation states behave as partially confined guided modes rather than radiation modes and are called *leaky modes*.[5,6,12,13] These leaky modes can travel considerable distances along a fiber but lose power through leakage or tunneling into the cladding as they propagate.

An important parameter connected with the cutoff condition is the *V number* defined by

$$V = \frac{2\pi a}{\lambda}\left(n_1^2 - n_2^2\right)^{1/2} = \frac{2\pi a}{\lambda}\text{NA} \tag{2.27}$$

This parameter is a dimensionless number that determines how many modes a fiber can support. Except for the lowest-order HE_{11} mode, each mode can exist only for values of V that exceed a certain limiting value (with each mode having a different V limit). The modes are cut off when $\beta = n_2k$. This occurs when $V \leq 2.405$. The HE_{11} mode has no cutoff and ceases to exist only when the core diameter is zero. This is the principle on which single-mode fibers are based. The details for these and other modes

The V number also can be used to express the number of modes M in a multimode step-index fiber when V is large (see Sec. 2.6 for modes in a graded-index multimode fiber). For this case, an estimate of the total number of modes supported in such a fiber is

$$M \approx \frac{1}{2}\left(\frac{2\pi a}{\lambda}\right)^2\left(n_1^2 - n_2^2\right) = \frac{V^2}{2} \tag{2.28}$$

Since the field of a guided mode extends partly into the cladding, as shown in Fig. 2.19, a final quantity of interest for a step-index fiber is the fractional power flow in the core and cladding for a given mode. As the V number approaches cutoff for any particular mode, more of the power of that mode is in the cladding. At the cutoff point, the mode becomes radiative with all the optical power of the mode residing in the cladding. Far from cutoff—that is, for large values of V—the fraction of the average optical power residing in the cladding can be estimated by

$$\frac{P_{\text{clad}}}{P} \approx \frac{4}{3\sqrt{M}} \tag{2.29}$$

where P is the total optical power in the fiber. The details for the power distribution between the core and the cladding of various LP_{jm} modes are given in Sec. 2.4.9. Note that since M is proportional to V^2, the power flow in the cladding decreases as V increases. However, this increases the number of modes in the fiber, which is not desirable for a high-bandwidth capability.

b)

Solution: Using the condition that $V \leq 2.405$ must be satisfied for single-mode operation, then from Eq. (2.27) we have

$$a = \frac{V\lambda}{2\pi}\frac{1}{\sqrt{n_1^2 - n_2^2}}$$

$$\leq \frac{2.405 \times 1.55\mu\text{m}}{2\pi}\frac{1}{\sqrt{(1.480)^2 - (1.478)^2}} = 7.7\mu\text{m}$$

If this fiber also should be single-mode at 1310 nm, then the core radius must be less than 6.50 μm.

2. With optical ray diagram, define numerical aperture (NA) and state its significance. Derive the expression for NA and acceptance angle for single mode step index fiber. [10] CO1 L2

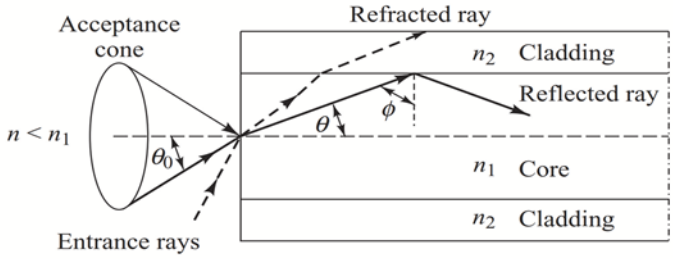

Fig. 2.17 *Meridional ray optics representation of the propagation mechanism in an ideal step-index optical waveguide*

The meridional ray is shown in Fig. 2.17 for a step-index fiber. The light ray enters the fiber core from a medium of refractive index n at an angle θ_0 with respect to the fiber axis and strikes the core-cladding interface at a normal angle ϕ. If it strikes this interface at such an angle that it is totally internally reflected, then the meridional ray follows a zigzag path along the fiber core, passing through the axis of the guide after each reflection.

From Snell's law, the minimum or critcal angle ϕ_c that supports total internal reflection for the meridional ray is given by

$$\sin \phi_c = \frac{n_2}{n_1} \tag{2.21}$$

Rays striking the core-cladding interface at angles less than ϕ_c will refract out of the core and be lost in the cladding, as the dashed line shows. By applying Snell's law to the air–fiber face boundary, the condition of Eq. (2.21) can be related to the maximum entrance angle $\theta_{0,\max}$, which is called the *acceptance angle* θ_A, through the relationship

$$n \sin \theta_{0,\max} = n \sin \theta_A = n_1 \sin \theta_c = \left(n_1^2 - n_2^2\right)^{1/2} \tag{2.22}$$

where $\theta_c = \pi/2 - \phi_c$. Thus those rays having entrance angles θ_0 less than θ_A will be totally internally reflected at the core–cladding interface. Thus θ_A defines an acceptance cone for an optical fiber.

Equation (2.22) also defines the *numerical aperture* (NA) of a step-index fiber for meridional rays:

$$\text{NA} = n \sin \theta_A = \left(n_1^2 - n_2^2\right)^{1/2} \approx n_1 \sqrt{2\Delta} \tag{2.23}$$

The approximation on the right-hand side is valid for the typical case where Δ, as defined by Eq. (2.20), is much less than 1. Since the numerical aperture is related to the acceptance angle, it is commonly used to describe the light acceptance or gathering capability of a fiber and to calculate source-to-fiber optical power coupling efficiencies. This is detailed in Chapter 5. The numerical aperture is a dimensionless quantity which is less than unity, with values normally ranging from 0.14 to 0.50.

3. Discuss the following for optical fibers: [10] CO1 L2
   a) Fiber bending loss
   b) Scattering loss

3.1.4 Bending Losses

Radiative losses occur whenever an optical fiber undergoes a bend of finite radius of curvature.[17–26] Fibers can be subject to two types of curvatures: (*a*) macroscopic bends having radii that are large compared with the fiber diameter, such as those that occur when a fiber cable turns a corner, and (*b*) random microscopic bends of the fiber axis that can arise when the fibers are incorporated into cables.

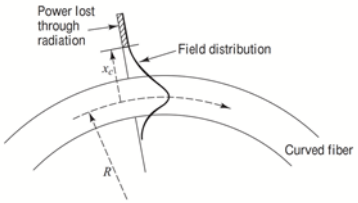

Fig. 3.7 *Sketch of the fundamental mode field in a curved optical waveguide. (Reproduced with permission from E.A.J. Marcatili and S. E. Miller,* Bell Sys. Tech. J., *vol. 48, p. 2161, Sept. 1969, © 1969, AT&T.)*

Let us first examine large-curvature radiation losses, which are known as *macrobending losses* or simply *bending losses*. For slight bends the excess loss is extremely small and is essentially unobservable. As the radius of curvature decreases, the loss increases exponentially until at a certain critical radius the curvature loss becomes observable. If the bend radius is made a bit smaller once this threshold point has been reached, the losses suddenly become extremely large.

Qualitatively, these curvature loss effects can be explained by examining the modal electric field distributions shown in Fig. 2.19. Recall that this figure shows that any bound core mode has an evanescent field tail in the cladding that decays exponentially as a function of distance from the core. Since this field tail moves along with the field in the core, part of the energy of a propagating mode travels in the fiber cladding. When a fiber is bent, the field tail on the far side of the center of curvature must move faster to keep up with the field in the core, as is shown in Fig. 3.7 for the lowest-order fiber mode. At a certain critical distance x_c from the center of the fiber, the field tail would have to move faster than the speed of light to keep up with the core field. Since this is not possible, the optical energy in the field tail beyond x_c radiates away.

The amount of optical radiation from a bent fiber depends on the field strength at x_c and on the radius of curvature R. Since higher-order modes are bound less tightly to the fiber core than lower-order modes, the higher-order modes will radiate out of the fiber first. Thus the total number of modes that can be supported by a curved fiber is less than in a straight fiber. The following expression[18] has been derived for the effective number of modes M_{eff} that are guided by a curved multimode fiber of radius a:

$$M_{\text{eff}} = M_{\infty}\left\{1 - \frac{\alpha+2}{2\alpha\Delta}\left[\frac{2a}{R} + \left(\frac{3}{2n_2 kR}\right)^{2/3}\right]\right\} \tag{3.7}$$

where α defines the graded-index profile, Δ is the core-cladding index difference, n_2 is the cladding refractive index, $k = 2\pi/\lambda$ is the wave propagation constant, and

$$M_{\infty} = \frac{\alpha}{\alpha+2}(n_1 ka)^2\Delta \tag{3.8}$$

is the total number of modes in a straight fiber [see Eq. (2.81)].

Another form of radiation loss in optical waveguide results from mode coupling caused by random microbends of the optical fiber.[27–30] *Microbends* are repetitive small-scale fluctuations in the radius of curvature of the fiber axis, as is illustrated in Fig. 3.8. They are caused either by nonuniformities in the manufacturing of the fiber or by nonuniform lateral pressures created during the cabling of the fiber. The latter effect is often referred to as *cabling* or *packaging losses.* An increase in attenuation results from microbending because the fiber curvature causes repetitive coupling of energy between the guided modes and the leaky or nonguided modes in the fiber.

One method of minimizing microbending losses is by extruding a compressible jacket over the fiber. When external forces are applied to this configuration, the jacket will be deformed but the fiber will

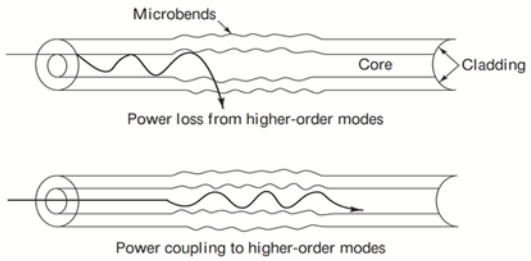

Fig. 3.8 *Small-scale fluctuations in the radius of curvature of the fiber axis lead to microbending losses. Microbends can shed higher-order modes and can cause power from low-order modes to couple to higher-order modes.*

tend to stay relatively straight. For a multimode graded-index fiber having a core radius a, outer radius b (excluding the jacket), and index difference Δ, the microbending loss α_M of a jacketed fiber is reduced from that of an unjacketed fiber by a factor[31]

$$F(\alpha_M) = \left[1 + \pi\Delta^2\left(\frac{b}{a}\right)^4\frac{E_f}{E_j}\right]^{-2} \tag{3.9}$$

Here, E_j and E_f are the Young's moduli of the jacket and fiber, respectively. The Young's modulus of common jacket materials ranges from 20 to 500 MPa. The Young's modulus of fused silica glass is about 65 GPa.

3.1.3 Scattering Losses

Scattering losses in glass arise from microscopic variations in the material density, from compositional fluctuations, and from structural inhomogeneities or defects occurring during fiber manufacture. As Sec. 2.7 describes, glass is composed of a randomly connected network of molecules. Such a structure naturally contains regions in which the molecular density is either higher or lower than the average density in the glass. In addition, since glass is made up of several oxides, such as SiO_2, GeO_2, and P_2O_5, compositional fluctuations can occur. These two effects give rise to refractive-index variations that occur within the glass over distances that are small compared with the wavelength. These index variations cause a Rayleigh-type scattering of the light. Rayleigh scattering in glass is the same phenomenon that scatters light from the sun in the atmosphere, thereby giving rise to a blue sky.

The expressions for scattering-induced attenuation are fairly complex owing to the random molecular nature and the various oxide constituents of glass. For single-component glass the scattering loss at a wavelength λ (given in μm) resulting from density fluctuations can be approximated by[3,14] (in base e units)

$$\alpha_{\text{scat}} = \frac{8\pi^3}{3\lambda^4}\,(n^2-1)^2\,k_B T_f \beta_T \tag{3.4a}$$

Here, n is the refractive index, k_B is Boltzmann's constant, β_T is the isothermal compressibility of the material, and the fictive temperature T_f is the temperature at which the density fluctuations are frozen into the glass as it solidifies (after having been drawn into a fiber). Alternatively, the relation[3,15] (in base e units)

$$\alpha_{\text{scat}} = \frac{8\pi^3}{3\lambda^4}\,n^8 p^2 k_B T_f \beta_T \tag{3.4b}$$

has been derived, where p is the photoelastic coefficient. A comparison of Eqs. (3.4*a*) and (3.4*b*) is given in Prob. 3.6. Note that Eqs. (3.4*a*) and (3.4*b*) are given in units of *nepers* (that is, base e units). As shown in Eq. (3.1), to change this to decibels for optical power attenuation calculations, multiply these equations by 10 log e = 4.343.

For multicomponent glasses the scattering at a wavelength λ (measured in μm) is given by[3]

$$\alpha = \frac{8\pi^3}{3\lambda^4}(\delta n^2)^2\,\delta V \tag{3.5}$$

where the square of the mean-square refractive-index fluctuation $(\delta n^2)^2$ over a volume of δV is

$$(\delta n^2)^2 = \left(\frac{\partial n^2}{\partial \rho}\right)^2 (\delta\rho)^2 + \sum_{i=1}^{m}\left(\frac{\partial n^2}{\partial C_i}\right)(\delta C_i)^2 \tag{3.6}$$

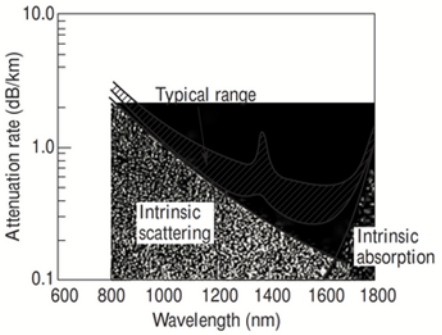

Fig. 3.5 *Typical spectral attenuation range for production-run graded-index multimode fibers. (Reproduced with permission from Keck,[16] © 1985, IEEE.)*

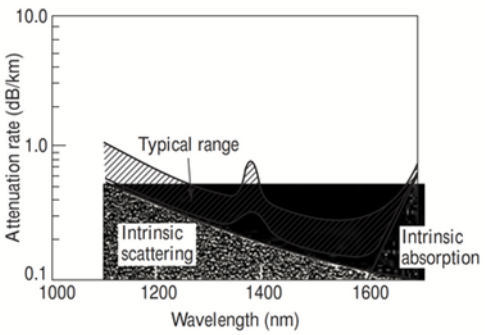

Fig. 3.6 *Typical spectral attenuation range for production-run single-mode fibers. (Reproduced with permission from Keck,[16] © 1985, IEEE.)*

Here, $\delta\rho$ is the density fluctuation and δC_i, is the concentration fluctuation of the ith glass component. Their magnitudes must be determined from experimental scattering data. The factors $\partial n^2/\partial\rho$ and $\partial n^2/\partial C_i$ are the variations of the square of the index with respect to the density and the ith glass component, respectively.

Structural inhomogeneities and defects created during fiber fabrication can also cause scattering of light out of the fiber. These defects may be in the form of trapped gas bubbles, unreacted starting materials, and crystallized regions in the glass. In general, the preform manufacturing methods that have evolved have minimized these extrinsic effects to the point where scattering that results from them is negligible compared with the intrinsic Rayleigh scattering.

Since Rayleigh scattering follows a characteristic λ^{-4} dependence, it decreases dramatically with increasing wavelength, as is shown in Fig. 3.3. For wavelengths below about 1 μm it is the dominant loss mechanism in a fiber and gives the attenuation-versus-wavelength plots their characteristic downward trend with increasing wavelength. At wavelengths longer than 1 μm, infrared absorption effects tend to dominate optical signal attenuation.

Combining the infrared, ultraviolet, and scattering losses, we get the results shown in Fig. 3.5 for multimode fibers and Fig. 3.6 for single-mode fibers.[16] Both of these figures are for typical commercial-grade silica fibers. The losses of multimode fibers are generally higher than those of single-mode fibers. This is a result of higher dopant concentrations and the accompanying larger scattering loss due to greater compositional fluctuation in multimode fibers. In addition, multimode fibers are subject to higher-order-mode losses owing to perturbations at the core-cladding interface.

4. Explain Intermodal dispersion with necessary equations. [10] CO1 L2

3.2.2 Modal Delay

Intermodal dispersion or *modal delay* appears only in multimode fibers. This signal-distorting mechanism is a result of each mode having a different value of the group velocity at a single frequency. To see why the delay arises, consider the meridional ray picture given in Fig. 2.17 for a multimode step-index fiber. The steeper the angle of propagation of the ray congruence, the higher is the mode number and, consequently, the slower the axial group velocity. This variation in the group velocities of the different modes results in a group delay spread, which is the intermodal dispersion. This dispersion mechanism is eliminated by single-mode operation but is important in multimode fibers. The maximum pulse broadening arising from the modal delay is the difference between the travel time T_{max} of the longest ray congruence paths (the highest-order mode) and the travel time T_{min} of the shortest ray congruence paths (the fundamental mode). This broadening is simply obtained from ray tracing and for a fiber of length L is given by

$$\Delta T = T_{max} - T_{min} = \frac{n_1}{c}\left(\frac{L}{\sin\varphi_c} - L\right) = \frac{L n_1^2}{c n_2}\Delta \tag{3.13}$$

where from Eq. (2.21) $\sin\varphi_c = n_2/n_1$ and Δ is the index difference.

The question now arises as to what maximum bit rate B can be sent over a multimode step-index fiber. Typically the fiber capacity is specified in terms of the *bit rate-distance product* BL, that is, the bit rate times the possible transmission distance L. In order for neighboring signal pulses to remain distinguishable at the receiver, the pulse spread should be less than $1/B$, which is the width of a bit period. For example,

a stringent requirement for a high-performance link might be $\Delta T \leq 0.1/B$. In general, we need to have $\Delta T < 1/B$. Using Eq. (3.13) this inequality gives the bit rate-distance product

$$BL < \frac{n_2}{n_1^2}\frac{c}{\Delta}$$

Taking values of $n_1 = 1.480$, $n_2 = 1.465$, and $\Delta = 0.01$, the capacity of this multimode step-index fiber is $BL = 20$ Mb/s-km.

The root-mean-square (rms) value of the time delay is a useful parameter for assessing the effect of modal delay in a multimode fiber. If it is assumed that the light rays are uniformly distributed over the acceptance angles of the fiber, then the rms impulse response σ_s due to intermodal dispersion in a step-index multimode fiber can be estimated from the expression

$$\sigma_s \approx \frac{L n_1 \Delta}{2\sqrt{3}c} \approx \frac{L(NA)^2}{4\sqrt{3}n_1 c} \tag{3.14a}$$

Here L is the fiber length and NA is the numerical aperture. Equation (3.14*a*) shows that the pulse broadening is directly proportional to the core-cladding index difference and the length of the fiber.

A successful technique for reducing modal delay in multimode fibers is through the use of a graded refractive index in the fiber core, as shown in Fig. 2.15. In any multimode fiber the ray paths associated with higher-order modes are concentrated near the edge of the core and thus follow a longer path through the fiber than lower-order modes (which are concentrated near the fiber axis). However, if the core has a graded index, then the higher-order modes encounter a lower refractive index near the core edge. Since the speed of light in a material depends on the refractive index value, the higher-order modes travel faster in the outer core region than those modes that propagate through a higher refractive index along the fiber center. Consequently this reduces the delay difference between the fastest and slowest modes. A detailed

analysis using electromagnetic mode theory gives the following absolute modal delay at the output of a graded-index fiber that has a parabolic ($\alpha = 2$) core index profile (see Sec. 2.6):

$$\sigma_s \approx \frac{L n_1 \Delta^2}{20\sqrt{3}c} \tag{3.14b}$$

Thus for an index difference of $\Delta = 0.01$, the theoretical improvement factor for intermodal rms pulse broadening in a graded-index fiber is 1000.

In graded-index fibers, careful selection of the radial refractive-index profile can lead to bit rate-distance products of up to 1 Gb/s-km.

5. Explain Fabry Perot resonator cavity of LASER with necessary diagrams and equations. [10] CO2 L2

Stimulated emission in semiconductor lasers arises from optical transitions between distributions of energy states in the valence and conduction bands. This differs from gas and solid-state lasers, in which radiative transitions occur between discrete isolated atomic or molecular levels. The radiation in one type of laser diode configuration is generated within a Fabry-Perot resonator cavity,[16–18] shown in Fig. 4.18, as in most other types of lasers. Here the cavity is approximately 250–500 μm long, 5–15 μm wide, and 0.1–0.2 μm thick. These dimensions commonly are referred to as the *longitudinal*, *lateral*, and *transverse dimensions* of the cavity, respectively.

As illustrated in Fig. 4.19, two flat, partially reflecting mirrors are directed toward each other to enclose the Fabry-Perot resonator cavity. The mirror facets are constructed by making two parallel clefts along natural cleavage planes of the semiconductor crystal. The purpose of the mirrors is to establish a strong optical feedback in the longitudinal direction. This feedback mechanism converts the device into an oscillator (and hence a light emitter) with a gain mechanism that compensates for optical losses in the cavity at certain resonant optical frequencies. The sides of the cavity are simply formed by roughing the edges of the device to reduce unwanted emissions in the lateral directions.

As the light reflects back and forth within the Fabry-Perot cavity, the electric fields of the light interfere on successive round trips. Those wavelengths that are integer multiples of the cavity length interfere constructively so that their amplitudes add when they exit the device through the right-hand facet. All other wavelengths interfere destructively and thus cancel themselves out. The optical frequencies at which constructive interference occurs are the *resonant frequencies* of the cavity. Consequently, spontaneously emitted photons that have wavelengths at these resonant frequencies reinforce themselves after multiple trips through the cavity so that their optical field becomes very strong. The resonant wavelengths are called the *longitudinal modes* of the cavity because they resonate along the length of the cavity.

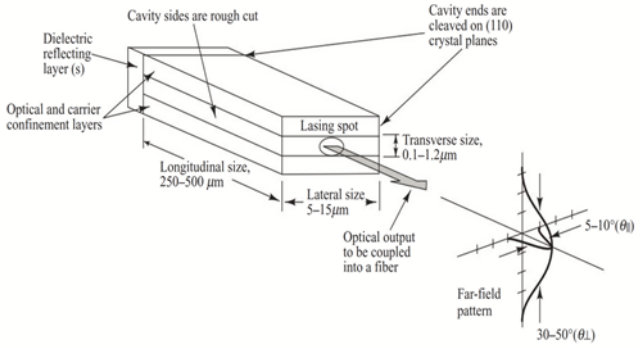

Fig. 4.18 *Fabry-Perot resonator cavity for a laser diode. The cleaved crystal ends function as partially reflecting mirrors. The unused end (the rear facet) can be coated with a dielectric reflector to reduce optical loss in the cavity. Note that the light beam emerging from the laser forms a vertical ellipse, even though the lasing spot at the active-area facet is a horizontal ellipse.*

Figure 4.20 illustrates the behavior of the resonant wavelengths for three values of the mirror reflectivity. The plots give the relative intensity as a function of the wavelength relative to the cavity length. As can be seen from Fig. 4.20, the width of the resonances depends on the value of the reflectivity. That is, the resonances become sharper as the reflectivity increases. Chapter 10 provides further details on the operational theory of Fabry-Perot cavities or etalons.

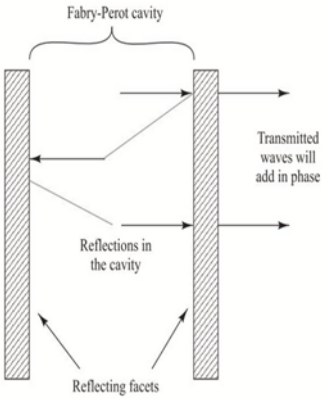

Fig. 4.19 *Two parallel light-reflecting mirrored surfaces define a Fabry-Perot resonator cavity.*

In another laser diode type, commonly referred to as the *distributed-feedback* (DFB) laser,[1,28,29] the cleaved facets are not required for optical feedback. A typical DFB laser configuration is shown in Fig. 4.21. The fabrication of this device is similar to the Fabry-Perot types, except that the lasing action is obtained from Bragg reflectors (gratings) or periodic variations of the refractive index (called *distributed-feedback corrugations*), which are incorporated into the multilayer structure along the length of the diode. This is discussed in more detail in Sec. 4.3.6.

In general, the full optical output is needed only from the front facet of the laser—that is, the one to be aligned with an optical fiber. In this case, a dielectric reflector can be deposited on the rear laser facet to reduce the optical loss in the cavity, to reduce the threshold current density (the point at which lasing starts), and to increase the external quantum efficiency. Reflectivities greater than 98 percent have been achieved with a six-layer reflector.

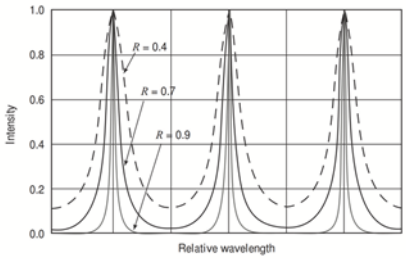

Fig. 4.20 *Behavior of the resonant wavelengths in a Fabry-Perot cavity for three values of the mirror reflectivity*

6. Explain internal quantum efficiency and power in detail for LED. [10] CO2 L2

4.2.3 Quantum Efficiency and LED Power

An excess of electrons and holes in *p*- and *n*-type material, respectively (referred to as *minority carriers*) is created in a semiconductor light source by carrier injection at the device contacts. The excess densities of electrons n and holes p are equal, since the injected carriers are formed and recombine in pairs in accordance with the requirement for charge neutrality in the crystal. When carrier injection stops, the carrier density returns to the equilibrium value. In general, the excess carrier density decays exponentially with time according to the relation

$$n = n_0 e^{-t/\tau} \tag{4.6}$$

where n_0 is the initial injected excess electron density and the time constant τ is the carrier lifetime. This lifetime is one of the most important operating parameters of an electro-optic device. Its value can range from milliseconds to fractions of a nanosecond depending on material composition and device defects.

The excess carriers can recombine either radiatively or nonradiatively. In radiative recombination a photon of energy $h\nu$, which is approximately equal to the bandgap energy, is emitted. Nonradiative recombination effects include optical absorption in the active region (self-absorption), carrier recombination at the heterostructure interfaces, and the Auger process in which the energy released during an electron–hole recombination is transferred to another carrier in the form of kinetic energy.

When there is a constant current flow into an LED, an equilibrium condition is established. That is, the excess density of electrons n and holes p is equal since the injected carriers are created and recombined in pairs such that charge neutrality is maintained within the device. The total rate at which carriers are generated is the sum of the externally supplied and the thermally generated rates. The externally supplied rate is given by J/qd, where J is the current density in A/cm^2, q is the electron charge, and d is the thickness of the recombination region. The thermal generation rate is given by n/τ. Hence, the rate equation for carrier recombination in an LED can be written as

$$\frac{dn}{dt} = \frac{J}{qd} - \frac{n}{\tau} \tag{4.7}$$

The equilibrium condition is found by setting Eq. (4.7) equal to zero, yielding

$$n = \frac{J\tau}{qd} \tag{4.8}$$

This relationship gives the steady-state electron density in the active region when a constant current is flowing through it.

The *internal quantum efficiency* in the active region is the fraction of the electron–hole pairs that recombine radiatively. If the radiative recombination rate is R_r and the nonradiative recombination rate is R_{nr}, then the internal quantum efficiency η_{int} is the ratio of the radiative recombination rate to the total recombination rate:

$$\eta_{int} = \frac{R_r}{R_r + R_{nr}} \tag{4.9}$$

For exponential decay of excess carriers, the radiative recombination lifetime is $\tau_r = n/R_r$ and the nonradiative recombination lifetime is $\tau_{nr} = n/R_{nr}$. Thus the internal quantum efficiency can be expressed as

$$\eta_{int} = \frac{1}{1 + \tau_r/\tau_{nr}} = \frac{\tau}{\tau_r} \tag{4.10}$$

where the *bulk recombination lifetime* τ is

$$\frac{1}{\tau} = \frac{1}{\tau_r} + \frac{1}{\tau_{nr}} \tag{4.11}$$

In general, τ_r and τ_{nr} are comparable for direct-bandgap semiconductors, such as GaAlAs and InGaAsP. This also means that R_r and R_{nr} are similar in magnitude, so that the internal quantum efficiency is about 50 percent for simple homojunction LEDs. However, LEDs having double-heterojunction structures can have quantum efficiencies of 60–80 percent. This high efficiency is achieved because the thin active regions of these devices mitigate the self-absorption effects, which reduces the nonradiative recombination rate.

If the current injected into the LED is I, then the total number of recombinations per second is

$$R_r + R_{nr} = I/q \tag{4.12}$$

Substituting Eq. (4.12) into Eq. (4.9) then yields $R_r = \eta_{int} I/q$. Noting that R_r is the total number of photons generated per second and that each photon has an energy $h\nu$, then the optical power generated internally to the LED is

$$P_{int} = \eta_{int} \frac{I}{q} h\nu = \eta_{int} \frac{hcI}{q\lambda} \tag{4.13}$$

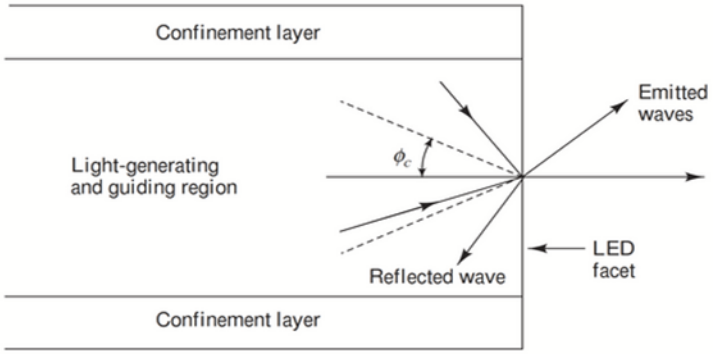

Fig. 4.15 *Only light falling within a cone defined by the critical angle ϕ_c will be emitted from an optical source.*

Not all internally generated photons will exit the device. To find the emitted power, one needs to consider the *external quantum efficiency* η_{ext}. This is defined as the ratio of the photons emitted from the LED to the number of internally generated photons. To find the external quantum efficiency, we need to take into account reflection effects at the surface of the LED. As shown in Fig. 4.15 and described in Sec. 2.2, at the interface of a material boundary only that fraction of light falling within a cone defined by the critical angle ϕ_c will cross the interface. From Eq. (2.18), we have that $\phi_c = \sin^{-1}(n_2/n_1)$. Here, n_1 is the refractive index of the semiconductor material and n_2 is the refractive index of the outside material, which nominally is air with $n_2 = 1.0$. The external quantum efficiency can then be calculated from the expression

$$\eta_{ext} = \frac{1}{4\pi}\int_0^{\phi_c} T(\phi)(2\pi\sin\phi)\,d\phi \tag{4.14}$$

where $T(\phi)$ is the *Fresnel transmission coefficient* or *Fresnel transmissivity*. This factor depends on the incidence angle ϕ, but, for simplicity, we can use the expression for normal incidence, which is[18,22]

$$T(0) = \frac{4n_1n_2}{(n_1+n_2)^2} \tag{4.15}$$

Assuming the outside medium is air and letting $n_1 = n$, we have $T(0) = 4n/(n+1)^2$. The external quantum efficiency is then approximately given by

$$\eta_{ext} \approx \frac{1}{n(n+1)^2} \tag{4.16}$$

From this, it follows that the optical power emitted from the LED is

$$P = \eta_{ext}P_{int} \approx \frac{P_{int}}{n(n+1)^2} \tag{4.17}$$

7. a. Consider a 30-km long optical fiber that has an attenuation of 0.4 dB/km at 1310 nm. Find the optical output power Pout if 200 mW of optical power is launched into the fiber. [06] CO1 L3

b. Consider a multimode step-index optical fiber that has a core radius of 25 µm, a core index of 1.48, and an index difference Δ = 0.01. The number of modes M = 760. Find the percentage of optical power that propagates in the cladding at 840 nm. [04] CO1 L3

a)

Example 3.2 As Sec. 1.3 describes, optical powers are commonly expressed in units of *dBm,* which is the decibel power level referred to 1 mW. Consider a 30-km long optical fiber that has an attenuation of 0.4 dB/km at 1310 nm. Suppose we want to find the optical output power P_{out} if 200 μW of optical power is launched into the fiber. We first express the input power in dBm units:

$$P_{in}(\text{dBm}) = 10\log\left[\frac{P_{in}(\text{W})}{1\,\text{mW}}\right]$$
$$= 10\log\left[\frac{200\times10^{-6}\ \text{W}}{1\times10^{-3}\,\text{W}}\right] = -7.0\ \text{dBm}$$

From Eq. (3.1*c*) with $P(0) = P_{in}$ and $P(z) = P_{out}$ the output power level (in dBm) at $z = 30$ km is

$$P_{out}(\text{dBm}) = 10\log\left[\frac{P_{out}(\text{W})}{1\,\text{mW}}\right]$$
$$= 10\log\left[\frac{P_{in}(\text{W})}{1\,\text{mW}}\right] - \alpha z$$
$$= -7.0\ \text{dBm} - (0.4\ \text{dB/km})\,(3\ 0\text{km})$$
$$= -19.0\ \text{dBm}$$

In unit of watts, the output power is

$$P(30\ \text{km}) = 10^{-19.0/10}(1\ \text{mW}) = 12.6\times10^{-3}\ \text{mW}$$
$$= 12.6\ \mu\text{W}$$

b)

Example 2.10 Consider a multimode step-index optical fiber that has a core radius of 25 μm, a core index of 1.48, and an index difference Δ = 0.01. Find the percentage of optical power that propagates in the cladding at 840 nm.

Solution: From Eqs. (2.23) and (2.28), at an operating wavelength of 840 nm the value of V is

$$V \approx \frac{2\pi a}{\lambda} n_1\sqrt{2\Delta} = \frac{2\pi\times25\,\mu\text{m}\times1.48}{0.84\,\mu\text{m}}\sqrt{2\times0.01}$$
$$= 39$$

Using Eq. (2.28), the total number of modes is

$$M \approx \frac{V^2}{2} = 760$$

From Eq. (2.29) we have

$$\frac{P_{clad}}{P} \approx \frac{4}{3\sqrt{M}} = 0.05$$

Thus approximately 5 percent of the optical power propagates in the cladding. If Δ is decreased to 0.03 in order to lower the signal dispersion (see Chapter 3), then there are 242 modes in the fiber and about 9 percent of the power propagates in the cladding.